# Blast Parameters from Cylindrical Charges Detonated
## on the Surface of the Ground

G. Guerke, G. Scheklinski-Glueck
Ernst-Mach-Institut, Freiburg
Germany

## Abstract

Tables and diagrams of scaled side-on blast parameters
are available for time of shock front arrival, primary
shock front overpressure, overpressure impulse and positive
duration for cylindrical RDX explosives having length to
diameter ratios of 1 and 5. Charges were placed in a vertical,
a horizontal and a $60^\circ$ inclined position to the surface of
the ground. Initiation point was at one end. Blast parameters
were measured along 9 blast lines at scaled standoffs from
0.5 to 32 $mkg^{-1/3}$.

*[handwritten annotation: to the minus 1/3 power]*

1. Introduction
2. Experimental Program
3. Scaling Law
4. Shock Front Contour
5. Blast Parameters as a Function of Azimuth Angle
6. Blast Parameters versus Scaled Distance
7. References

## 1. Introduction

The objective of this report is to present a compilation of blast data from a series of small scale HE tests with cylindrical charges detonated at the surface of the ground. In a literature search we found just one investigation concerning blast data of cylindrical charges fired on the ground surface (Ref. 1, 1975). In agreement with a recent manual for the prediction of blast loadings on structures (Ref. 3, 1980) we decided, that the existing data for explosions of elongated charges on the ground surface are not extensive enough to develop prediction curves and equations, and are not adequate to check scaling laws. Hence an experimental program was designed to gather more data on the blast from cylindrical charges fired on the surface of the ground oriented with the axis parallel, oblique and normal to the surface.

## 2. Experimental Program

The experimental program is delineated in Table 1. Cylindrical charges having length to diameter ratios of 1 and 5 were selected. Rounds were fired for each geometry with the charge in vertical position and with the initiation from the top (No. 4 in Table 1). In the next group, charges were placed in a horizontal position on the ground and detonated from one end (No. 1 in Table 1). Figure 2.1 shows a top plan of the cylindrical charge with the initiation point at the end in line with the 0 degree line. Keeping the charge fixed and moving clockwise we have the instrument line at 9 different azimuth angles H at 0, 22.5, 45, 67.5, 90, 112.5, 135, 157.5, 180 degrees to the ground zero point.

## Table 1     Test Plan

A three-number code is used to characterize the test
arrangement. Initiation point is at H = O. The code:
L/D ratio - Azimuth Angle H - Angle of Inclination V

1. Horizontal Cylinders (Angle of Inclination V = O)

```
5 -    0   - 0          1 -    0   - 0
5 -  22,5  - 0          1 -   45   - 0
5 -   45   - 0          1 -   90   - 0
5 -  67,5  - 0          1 - 112,5  - 0
5 -   90   - 0          1 - 135    - 0
5 - 112,5  - 0
5 - 135    - 0
5 - 157,5  - 0
5 - 180    - 0
```

2. 45 Degrees Inclined Cylinders

```
5 -    0   - 45         1 -    0   - 45
5 -   90   - 45         1 -   90   - 45
5 -  180   - 45         1 -  180   - 45
```

3. 60 Degrees Inclined Cylinders

```
5 -    0   - 60         1 -    0   - 60
5 -   45   - 60         1 -   90   - 60
5 -   90   - 60         1 -  180   - 60
5 -  135   - 60
5 -  180   - 60
```

4. Vertical Cylinders (Symmetric in azimuth angle)

```
5 -   S   - 90          1 -.  S   - 90
```
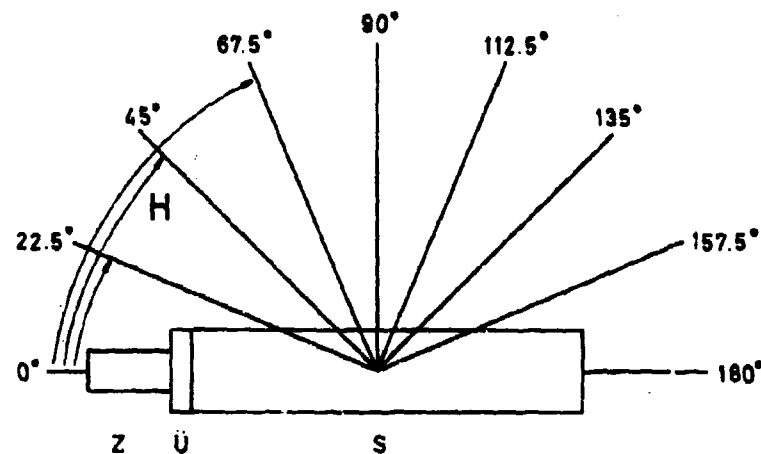
5. Hemispherical Charges

Fig. 2.1

Top Plan of Blast Lines at Azimuth Angles H.

Initiation Point at H = 0.

Z = Igniter   Ü = Propagation Charge
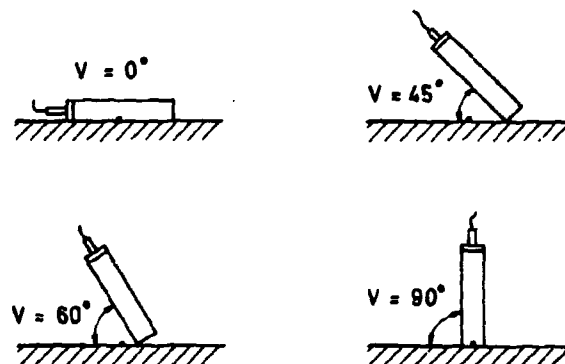
S = RDX cylinder



Fig. 2.2
Side View of Cylindrical Charges Inclined
to the Surface of the Ground

As Figure 2.2 shows each of the two L/D geometries was
fired in a position at vertical elevation V = 60° degrees
inclined to the ground surface with end initiation away
from the ground (No. 3 in Table 1). To complete the program
some rounds were fired in a position V = 45° degrees to the
ground surface (No. 2 in Table 1). Semispherical charges of
identical masses and identical type of HE were initiated
at their center of mass in order to  get reference values
for the semi-spherical blast propagation (No. 5 in Table 1).

All charges, as shown in Table 2, were bare RDX with
nominal weight of 0.016 kg, 0.128 kg and 1.024 kg.

<div align="center">

Table 2     Explosives Specifications
</div>

Cylindrical Charges S  94.5 % RDX

          4.5 % Wax

          1.0 % Graphite

Charge Density     1680 kg m$^{-3}$

Precision Microsecond Igniter PL 464 Dynamit Nobel

L = Charge Length  D = Charge Diameter  U = Propagation Charge

| Mass in kg | L/D = 1 | | L/D = 5 | | | |
|---|---|---|---|---|---|---|
| | D in cm | L in cm | D in cm | L in cm | U in g | S in g |
| 0.016 | 2,3 | 2,3 | 1,35 | 6,7 | 2 | 14 |
| 0.128 | 4,6 | 4,6 | 2,7 | 13,4 | 5 | 123 |
| 1.024 | 9,2 | 9,2 | 5,4 | 26,8 | 8 | 1016 |

Firings were made on heavy steel plates that were nearly
perfect reflectors of blast waves. Restoration of the plates
and of the compacted sand under them was carried out after
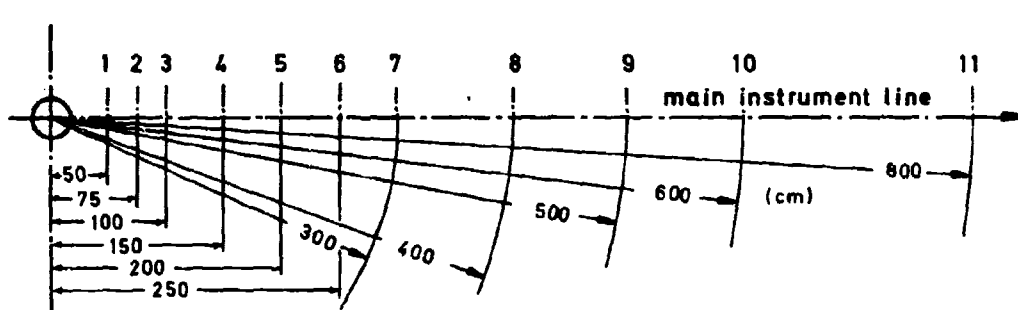each event. Shown in Figure 2.3 is the field layout.



Fig. 2.3
Top Plan of the Field Layout
Blast Gages No 1 to 11 along the Main Instrument
Line. All distances in centimeters

The geometric center or a projection thereof was used as the
ground zero point. Eleven blast gages were installed along
the main instrument line extending from 0.5 meter to 8 meter,
corresponding to scaled distances from $Z = 0.5$ to $Z = 32\,m\,kg^{-1/3}$
Two additional control gages were located at an off angle at
$90^{\circ}$ equal to station 2 at 0.75 meter and to station 4 at
1.5 meter. The pressure transducers were Kistler Instruments
model 603 B piezoelectric sensing elements having a natural

# Table 3

BLASTPARAMETER , ZYLINDRISCHE LADUNGEN    ANORDNUNG  5 - 90 - 0

| NR | Z | TA | PS | IS+ | T+ |
|----|-----|--------|--------|--------|--------|
| 1 | 0.50 | 1.17E-01 | 1 | 2.33E+00 | 1.99E-01 |
| 2 | 0.60 | 1.45E-01 | 1 | 2.33E+00 | 2.49E-01 |
| 3 | 0.70 | 1.74E-01 | 1 | 2.33E+00 | 3.02E-01 |
| 4 | 0.80 | 2.06E-01 | 1 | 2.38E+00 | 3.56E-01 |
| 5 | 1.00 | 2.74E-01 | 8.18E+01 | 2.88E+00 | 4.69E-01 |
| 6 | 1.25 | 3.70E-01 | 5.70E+01 | 2.83E+00 | 6.19E-01 |
| 7 | 1.50 | 4.78E-01 | 4.11E+01 | 2.83E+00 | 7.75E-01 |
| 8 | 1.75 | 5.97E-01 | 2.95E+01 | 2.88E+00 | 9.38E-01 |
| 9 | 2.00 | 7.28E-01 | 2.15E+01 | 2.89E+00 | 1.11E+00 |
| 10 | 2.25 | 8.71E-01 | 1.59E+01 | 2.02E+00 | 1.28E+00 |
| 11 | 2.50 | 1.02E+00 | 1.10E+01 | 2.85E+00 | 1.46E+00 |
| 12 | 2.75 | 1.27E+00 | 7.60E+00 | 2.29E+00 | 1.64E+00 |
| 13 | 3.00 | 1.56E+00 | 5.40E+00 | 1.87E+00 | 1.83E+00 |
| 14 | 3.50 | 2.24E+00 | 2.95E+00 | 1.31E+00 | 2.21E+00 |
| 15 | 4.00 | 3.07E+00 | 1.75E+00 | 9.09E-01 | 2.62E+00 |
| 16 | 4.50 | 4.05E+00 | 1.19E+00 | 7.91E-01 | 2.82E+00 |
| 17 | 5.00 | 5.27E+00 | 7.68E-01 | 6.99E-01 | 3.00E+00 |
| 18 | 5.50 | 6.32E+00 | 6.01E-01 | 6.25E-01 | 3.18E+00 |
| 19 | 6.00 | 7.43E+00 | 4.84E-01 | 5.64E-01 | 3.36E+00 |
| 20 | 7.00 | 9.79E+00 | 3.36E-01 | 4.70E-01 | 3.69E+00 |
| 21 | 8.00 | 1.23E+01 | 2.50E-01 | 4.02E-01 | 4.01E+00 |
| 22 | 9.00 | 1.50E+01 | 1.95E-01 | 3.50E-01 | 4.31E+00 |
| 23 | 10.00 | 1.77E+01 | 1.58E-01 | 3.09E-01 | 4.60E+00 |
| 24 | 11.00 | 2.05E+01 | 1.32E-01 | 2.76E-01 | 4.87E+00 |
| 25 | 12.00 | 2.34E+01 | 1.13E-01 | 2.49E-01 | 5.14E+00 |
| 26 | 14.00 | 2.92E+01 | 8.67E-02 | 2.08E-01 | 5.65E+00 |
| 27 | 16.00 | 3.51E+01 | 7.05E-02 | 1.77E-01 | 6.09E+00 |
| 28 | 18.00 | 4.09E+01 | 5.95E-02 | 1.54E-01 | 6.15E+00 |
| 29 | 20.00 | 4.66E+01 | 5.18E-02 | 1.76E-01 | 6.20E+00 |
| 30 | 22.00 | 5.22E+01 | 4.61E-02 | 1.22E-01 | 6.25E+00 |
| 31 | 24.00 | 5.77E+01 | 4.17E-02 | 1.10E-01 | 6.29E+00 |
| 32 | 28.00 | 6.82E+01 | 3.56E-02 | 9.18E-02 | 6.37E+00 |
| 33 | 32.00 | 7.80E+01 | 3.17E-02 | 7.84E-02 | 6.43E+00 |

KOEFFIZIENTEN DER AUSGLEICHSFUNKTION , ANORDNUNG  5 - 90 - 0

| | VON Z | BIS Z | GRAD | R SQU | B0 | B1 | B2 |
|-----|-------|-------|------|-------|--------|--------|--------|
| TA : | | | | | | | |
| | 0.50 | 2.50 | 2 | 0.998 | -0.5623 | 1.3159 | 0.3125 |
| | 2.50 | 5.00 | 1 | 1.000 | -0.9309 | 2.3556 | |
| | 5.00 | 32.00 | 2 | 1.000 | -0.9111 | 2.7476 | -0.5881 |
| PS : | | | | | | | |
| | 0.87 | 2.50 | 2 | 1.000 | 1.9129 | -1.3696 | -1.8590 |
| | 2.50 | 5.00 | 1 | 0.995 | 2.6033 | -3.9207 | |
| | 5.00 | 32.00 | 2 | 0.995 | 2.2610 | -4.1797 | 1.1172 |
| IS+ : | | | | | | | |
| | 0.50 | 2.50 | 1 | 0.000 | 0.4594 | 0 | |
| | 2.50 | 4.00 | 1 | 0.999 | 1.3691 | -2.2979 | |
| | 4.00 | 32.00 | 1 | 0.998 | 0.6682 | -1.1735 | |
| T+ : | | | | | | | |
| | 0.50 | 4.00 | 1 | 1.000 | -0.3286 | 1.2386 | |
| | 4.00 | 16.00 | 1 | 0.999 | 0.0483 | 0.6136 | |
| | 16.00 | 32.00 | 1 | 0.924 | 0.6389 | 0.0794 | |

frequency of 500 kc. Signals were recorded on Transient Re-
corders having a frequency bandpass 0 - 150 kc. The data
was reduced with the aid of a HP 9830 A desk computer.
Scaled arrival time $TA \cdot Q^{-1/3}$, shock front overpressure PS,
scaled overpressure impuls $IS \cdot Q^{-1/3}$ and scaled positive
duration $T \cdot Q^{-1/3}$ were obtained from more than 1200 records.

A final report covers the reduced data of the entire pro-
gram (Ref. 4). Interested people will find 35 Tables and 35
Diagrams in the report belonging to different charge orientat-
ions and directions of blast propagation (see Table 1).
One example is to be seen in Tab. 3, in order to show the
arrangement of data. At 33 values of the scaled distance
parameter Z the scaled blast parameters have been listed at
distances that allow linear interpolation. Also coefficients
of least-squares regression power functions of blast data as
a function of scaled distance have been listed. Blast data
can be taken from the tables directly for 1 kilogram charges
but must be multiplied by the cube root of the charge mass
for all charges heavier or lighter than 1 kilogram. A proce-
dure that is well known to people who handle TNT standard
curves or tables. Remember that the scaling of blast data
works correctly as long as the basic assumptions of Hopkinson-
Cranz scaling rules are fulfilled.

## 3. Scaling Laws

Tests were conducted at three different charge masses of RDX at identical charge geometries and identical test arrangements. Table 4 may show as an example that Cranz-Hopkinson scaling proofed well throughout our test series. Time of arrival data have been listed for the test-arrangement 1-90-0 (L/D = 1, charge axis parallel to the ground, direction of blast measurement 90°). Direct comparison of test results can be made at scaled distances between $Z = 2$ and $Z = 8$. Time-of-arrival measurements in milliseconds differ by a factor of about 4 between 16 gram and 1 kilogram charges, but scaled time-of-arrival data correspond within 3 per cent.

Table 4   Check of Scaling Laws
Time of Shock Front Arrival for 3 Different
Charge Masses. Test Arrangement 1-90-0

| $Z$ \ $Q$ | 0.016 kg | | | 0.128 kg | | | 1.024 kg | | |
|---|---|---|---|---|---|---|---|---|---|
| $R/Q^{1/3}$ | $R$ in m | $t_A$ in ms | $t_A/Q^{1/3}$ | $R$ in m | $t_A$ in ms | $t_A/Q^{1/3}$ | $R$ in m | $t_A$ in ms | $t_A/Q^{1/3}$ |
| 2 | 0.5 | 0.21 | 0.83 | 1 | 0.42 | 0.83 | 2 | 0.82 | 0.81 |
| 4 | 1 | 1.03 | 4.09 | 2 | 2.0 | 3.97 | 4 | 4.10 | 4.08 |
| 8 | 2 | 3.55 | 14.1 | 4 | 7.22 | 14.3 | 8 | 14.4 | 14.3 |

Fig. 3.1 shows just one example of measured pressure-
time histories at tests with different charge marses at
identical scaled distances. Time and impulse scales are
scaled to 1 kilogram. It is easily to be seen, that measure-
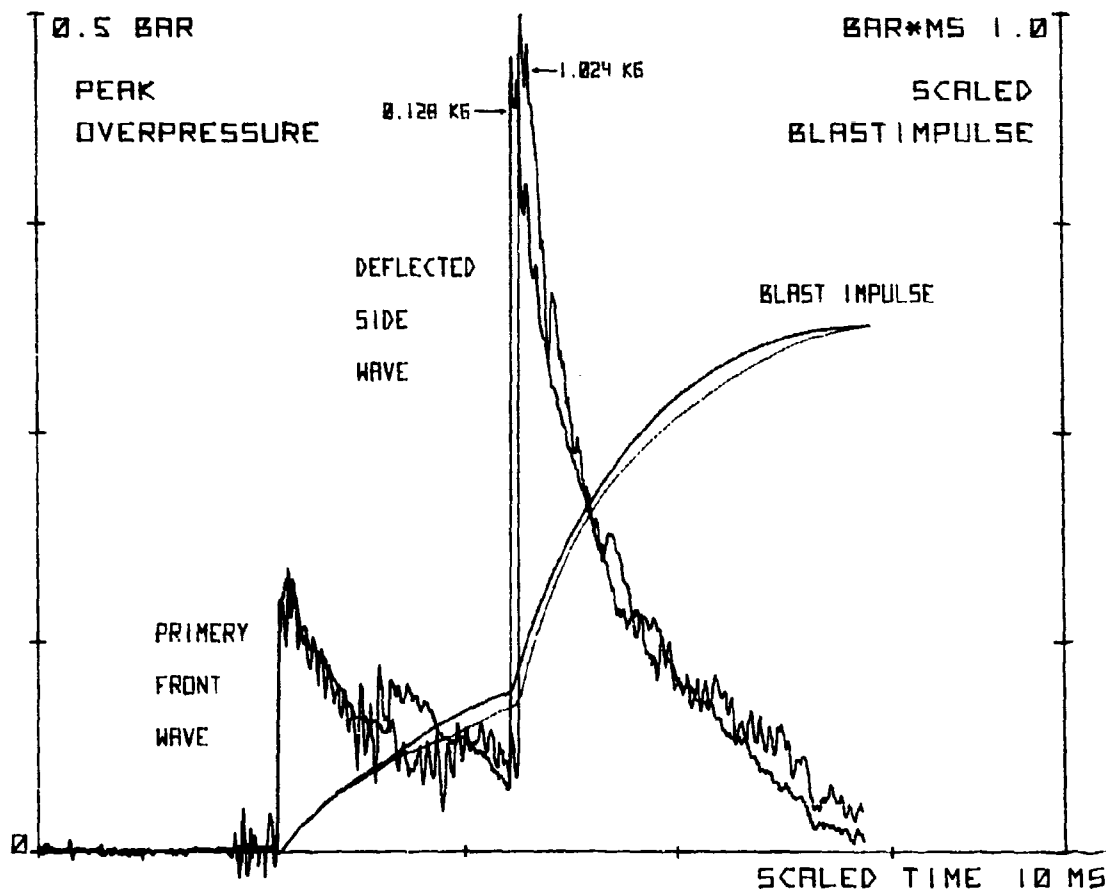ments are nearly identical.



FIG.3.1

PRESSURE-TIME RECORDS SCALED TO 1 KG-EQUIVALENT.

TEST ARRANGEMENT  S - 180 - 0

## 4. Shock Front Contour

For a charge of cylindrical geometry as standoff in-
creases the shock front becomes more spherical. This is shown
in Figures 4.1 to 4.3. Iso time of arrival lines that mark
the shock front contours are shown for 3 scaled arrival  times
TA 0.874; 5.6; 46.6 after ignition time. Semicircles mark
the shock front from semispherical charges at identical
arrival time. Peak overpressure is identical along the semi-
circles 7 bar (100 psi); 0.7 bar (10 psi); 0.07 bar (1 psi).
At the same instant after charge ignition the shock front
contour of the cylindrical charge is asymmetric with largest
distance from the explosion center at $90^\circ$, $112,5^\circ$ and $180^\circ$
(Fig. 4.1). The peak overpressure at the shock front is far
from uniform for cylindrical charges. It is given  in small
figures along the contour. High peak overpressure in $90^\circ$
direction in Fig. 4.1 is due to the side-wave and in $180^\circ$
it is due to the front wave. Highest peak overpressure in
$112,5^\circ$ direction is produced by the asymmetric ignition at
$0^\circ$. In that  case the detonation gas has a forward velocity
component that may cause the strongest shock not in $90^\circ$ but
in a forward direction. The falling back shock front and low
pressure  at $0^\circ$ to $45^\circ$ is produced by  asymmetric ignition.

The Figures 4.2 and 4.3 show that the shock front contour
becomes more spherical. But even in the far field, where semi-
spherical charges produce a peak overpressure of 0.07 bar
(1 psi), the cylindrical charge produces peak overpressures
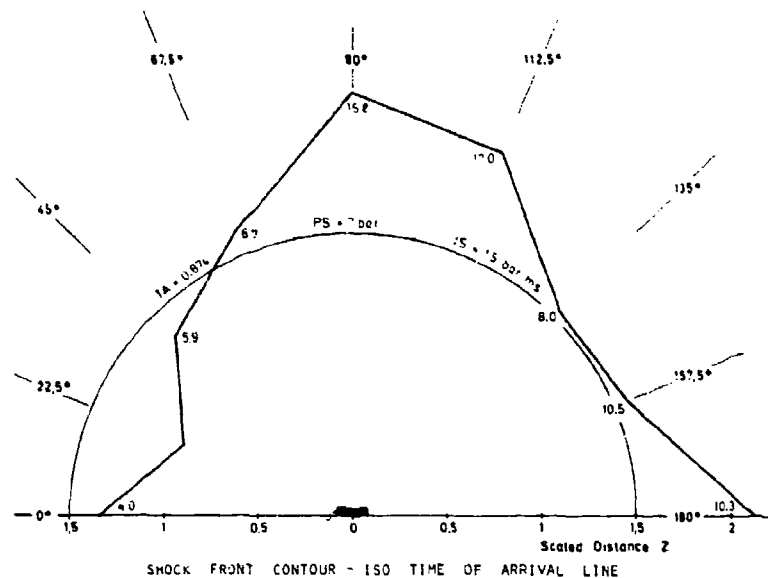from 0.05 to 0.1 bar at the shock front.

SHOCK FRONT CONTOUR - ISO TIME OF ARRIVAL LINE
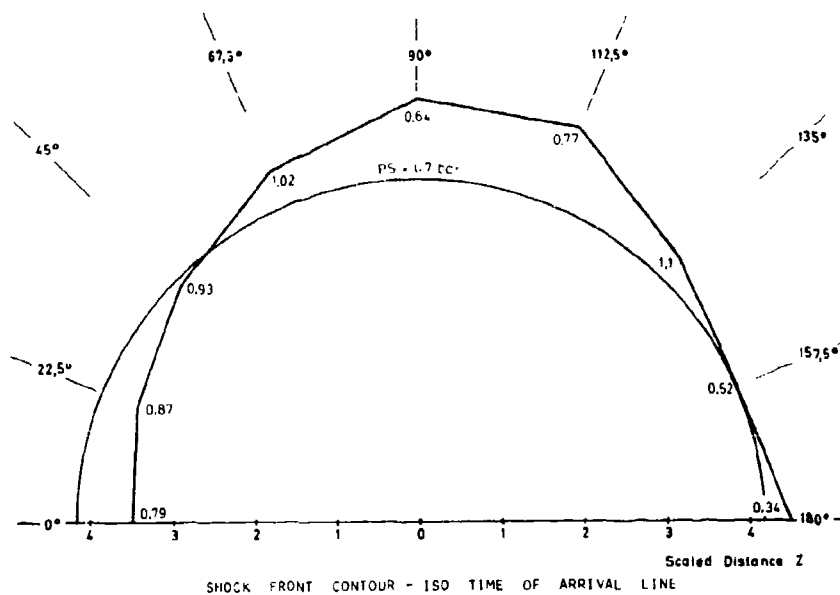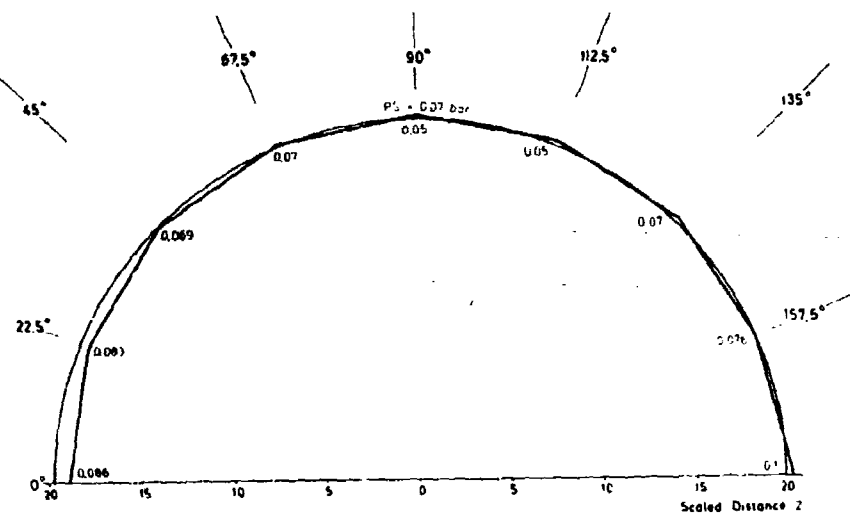
$$TA \; Q^{-1/3} = 0.874 \; MS \; KG^{-1/3}$$

FIG. 4.1

CYLINDRICAL RDX CHARGE L/D = 5; V = 0; IGNITION AT 0° VARIABLE SHOCK FRONT OVERPRESSURE ALONG THE ISO LINE. SEMICIRCLE: SHOCK FRONT CONTOUR FOR SEMISPHERICAL CHARGE OF IDENTICAL MASS. SCALED DISTANCE Z = 1.5. SHOCK FRONT OVERPRESSURE PS = 7 BAR.



SHOCK FRONT CONTOUR - ISO TIME OF ARRIVAL LINE

$$TA \; Q^{-1/3} = 5.6 \; MS \; KG^{-1/3}$$

FIG. 4.2

CYLINDRICAL RDX CHARGE L/D = 5; V = 0; IGNITION AT 0° VARIABLE SHOCK FRONT OVERPRESSURE ALONG THE ISO LINE. SEMICIRCLE: SHOCK FRONT CONTOUR FOR SEMISPHERICAL CHARGE OF IDENTICAL MASS. SCALED DISTANCE Z = 4.2. SHOCK FRONT OVERPRESSURE PS = 0.7 BAR.

SHOCK FRONT CONTOUR - ISO TIME OF ARRIVAL LINE

$$TA \ Q^{-1/3} = 46.6 \quad MS \quad KG^{-1/3}$$

FIG. 4.3
CYLINDRICAL RDX CHARGE L/D = 5 : V = 0 : IGNITION AT $0^O$ VARIABLE SHOCK
FRONT OVERPRESSURE ALONG THE ISO LINE. SEMICIRCLE: SHOCK FRONT CON-
TOUR FOR SEMISPHERICAL CHARGE OF IDENTICAL MASS. SCALED DISTANCE
Z = 20 SHOCK FRONT OVERPRESSURE PS = 0.07 BAR.

99

## 5. Blast Parameters as a Function of Azimuth Angle

If a hemispherical charge resting on a flat surface is
initiated at its center of mass a shock wave will travel
through the surrounding air, its strength a function of
radial standoff from the center of the explosion. For a cy-
lindrical charge that is initiated at one end the shock wave
will not enter the surrounding air as a spherical wave, nor
at the same time over the entire charge surface. The shape
and strength of the shock wave will depend upon the length
to diameter ratio, and upon the location at which initiation
occurred. The blast parameters will be functions not only of
radial standoff, but also of azimuth.

Figures 5.1 through 5.4 are plots comparing blast data
of cylindrical charges to hemispherical charges. Primary shock
front peak overpressure and positive pressure impulse are
plotted as a function of azimuth angle H and scaled distance Z,
for cylindrical charges having length to diameter ratios of
1 and 5. Our final report covers data from the entire program
(Lit. 4).
Results of semispherical charges are plotted as horizontal
lines. Azimuthal symmetry is valid at that case. Unsymmetrical
blast propagation around cylindrical charges is identified
very clearly at this type of diagram that has been used in
Ref. 3.

Figure 5.2a summarizes primary shock front overpressure
data in the near field at scaled distances from $Z = 1$ to
$Z = 2.5$ for $L/D = 5$. Maximum peak overpressure of about
150 bar at $Z = 1$ was measured in $H = 112.5^{\circ}$ direction. Former
investigators who had measuring lines at $90^{\circ}$ and $135^{\circ}$ could
not detect this effect of the asymmetric expansion of the
detonation gases as a consequence of ignition at $0^{\circ}$.

Minimum peak overpressure at Z = 1 occurred at H = 22.5$^{\circ}$
direction of about 5.5 bar as a consequence of asymmetric
ignition and the bridge wave phenomenon. Very high peak
overpressure was observed at Z = 1 at H = 180$^{\circ}$ direction as
an effect of the front wave. Errors of about a factor of
10 in peak overpressure may be induced in the near field by
neglecting the charge shape.

Most people think that blast parameters from non-spherical
charges smoothen continuously to spherical parameters in the
far field. In fact the peak overpressure from cylinders with
L/D = 5 seems to smoothen at scaled distance Z = 7 in figure
5.2b. Former investigator only measured up to this distance.
But far out can we recognize the effect that at distances
from Z = 10 to Z = 20 peak overpressure is very small at
H = 90$^{\circ}$ and H = 112.5$^{\circ}$ directions and high in H = 0$^{\circ}$ and
H = 180$^{\circ}$. This type of overreaction corresponds to reflection
and diffraction phenomena of primary side waves and end
waves from the cylindrical explosives. Pressure-distance re-
lationships are determined not only by one shock front, but
by side-waves, end-waves and bridge-waves that result in
multiple pressure peaks. Some wave fronts tend to heal by
overtaking and merging with the primary front while others
tend to recede. As a result even in the far field, at Z = 20,
errors of about a factor of 2 (100 percent) in peak over-
pressure are induced by neglecting the charge shape.

Figures 5.1a and 5.1b summarize peak overpressure data
from cylinders with L/D = 1. There are some remarkable differ-
ences between length to diameter ratios 5 and 1. All of them
can be qualitatively explained by the different charge geo-
metry and the observation that high peak overpressure in a
certain direction tends to fall down to very low pressure at
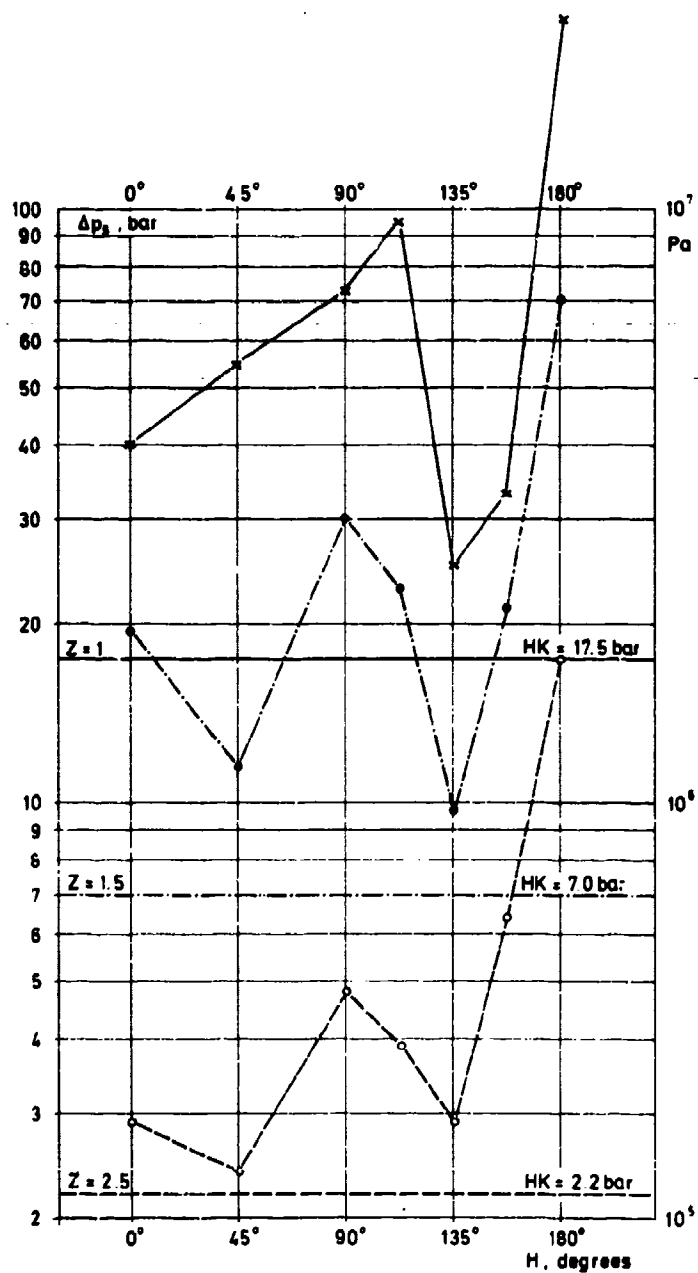increasing distances. The rate of change in peak overpressure

Fig 5.1a    Primary Shock Front Side-on Overpressure
as a Function of Azimuth Angle H and Scaled Distance
$Z = R \cdot Q^{-1/3}$ in mkg$^{-1/3}$ for Cylindrical Charges with
L/D Ratio of 1.   Horizontal Lines Indicate Shock Front
Overpressure of Semispherical Charges of Identical Mass
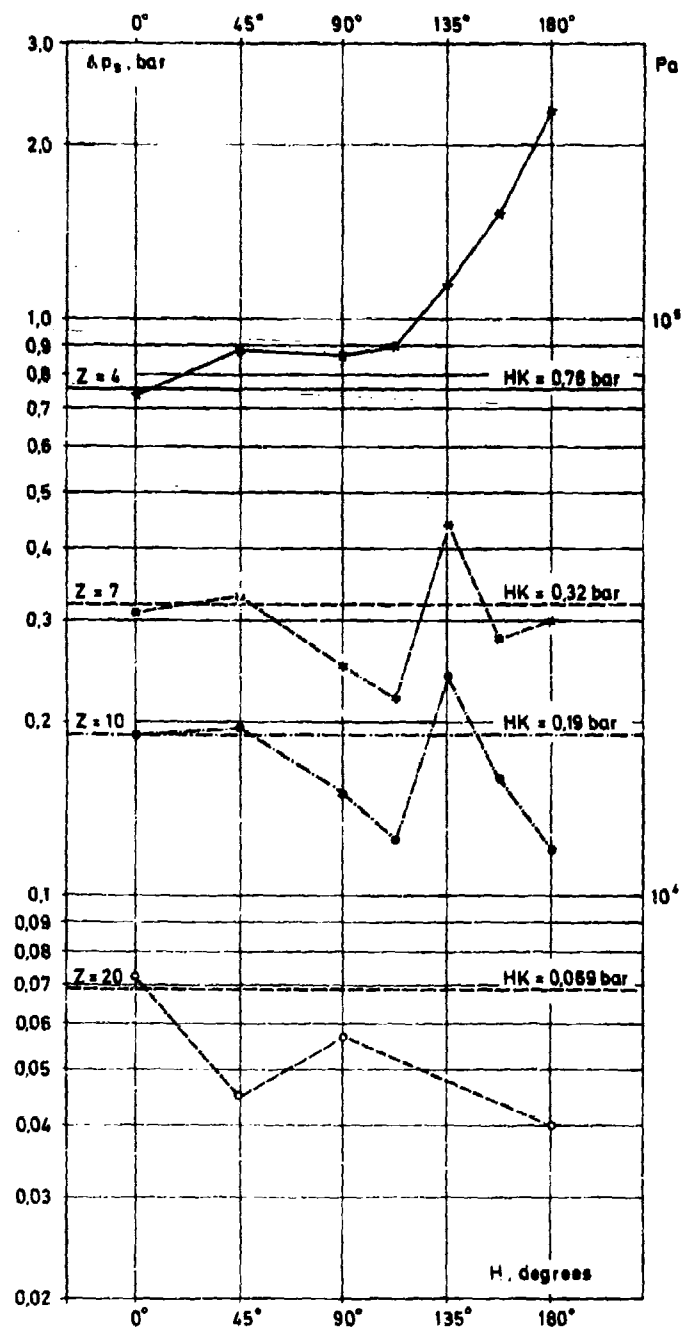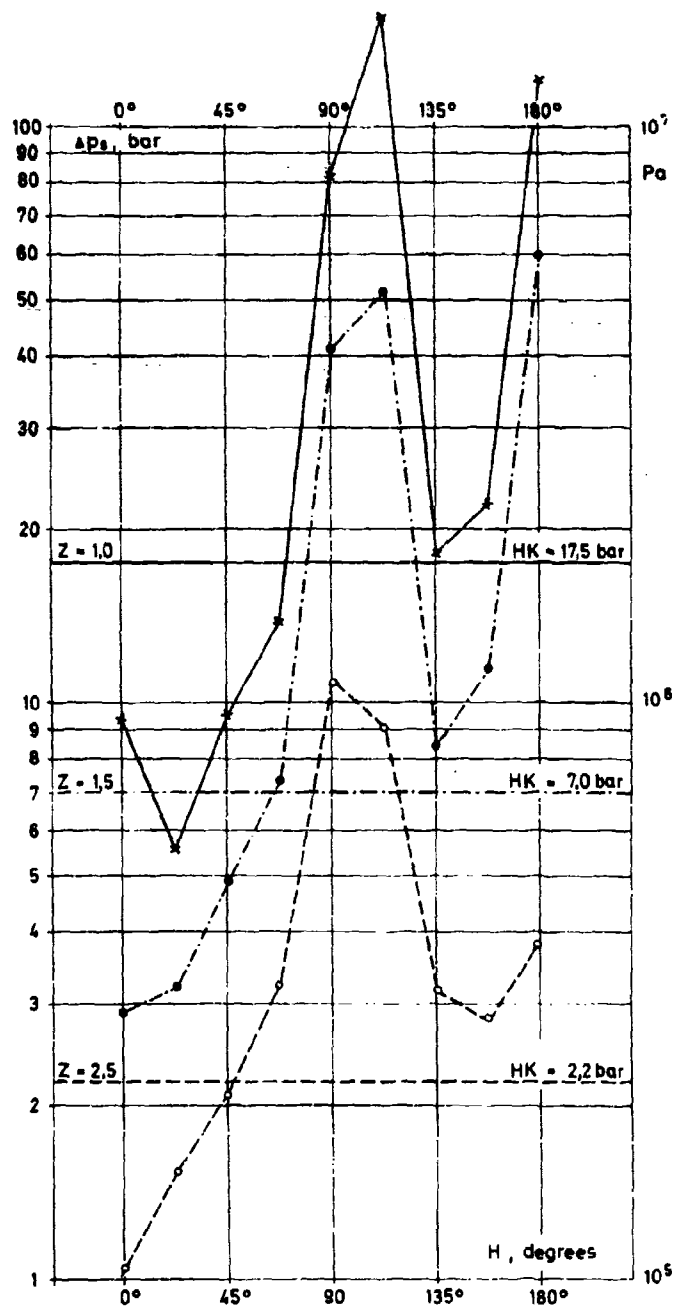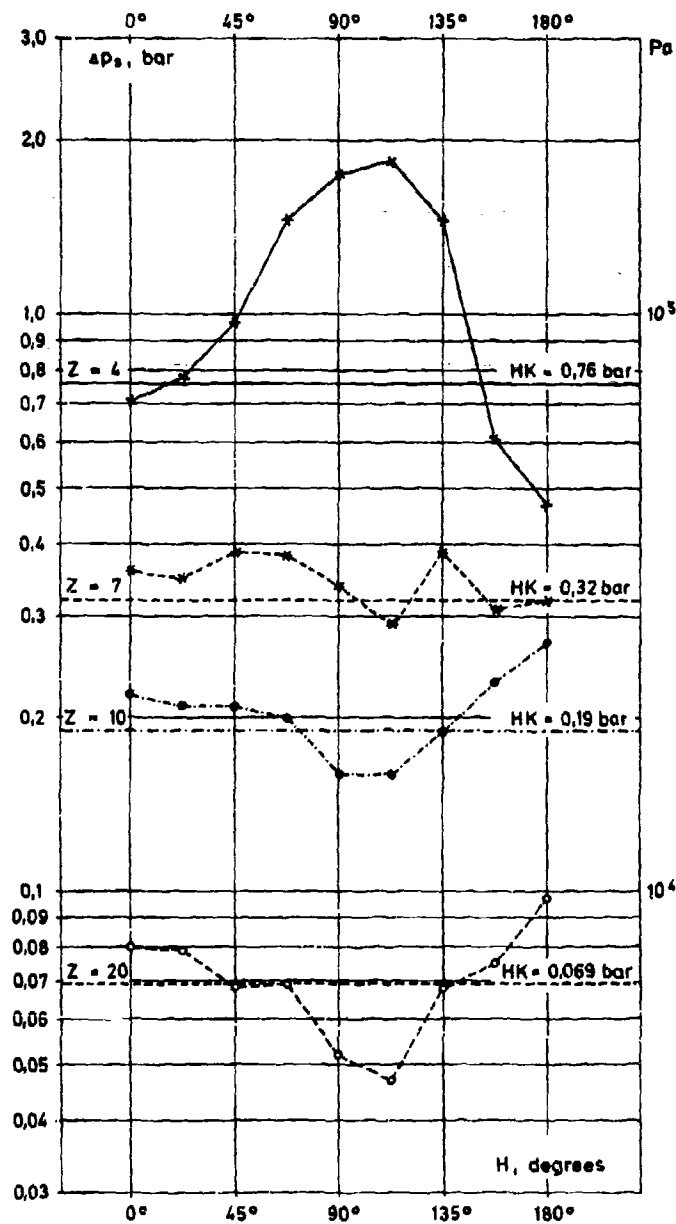at the Same Scaled Distance.

Fig. 5.1b    Primary Shock Front Side - on  Overpressure
as a Function of Azimuth Angle H and Scaled Distance
$Z = R \cdot Q^{-1/3}$  in  $mkg^{-1/3}$  for Cylindrical  Charges with
L/D Ratio of 1     Horizontal Lines Indicate Shock Front
Overpressure of Semispherical Charges of Identical Mass
at the Same Scaled  Distance.
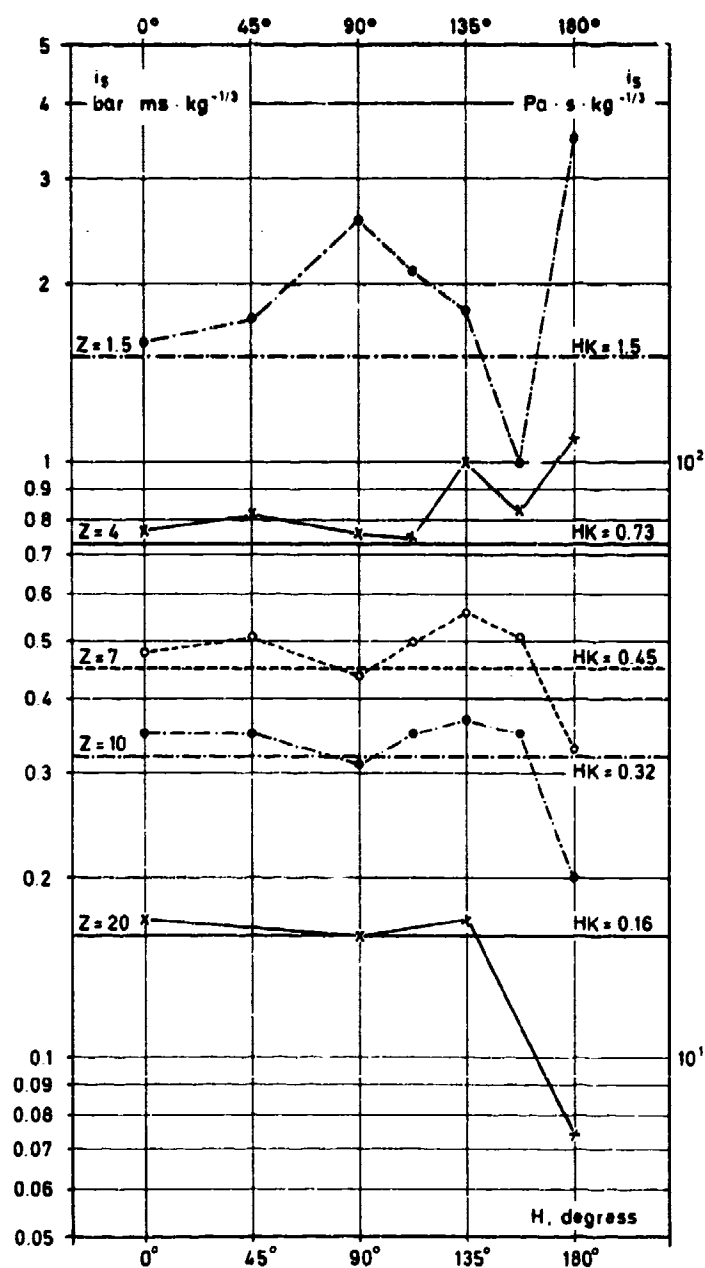
**Fig. 5.2a** Primary Shock Front Side-on Overpressure as a Function of Azimuth Angle H and Scaled Distance $Z = R \cdot Q^{-1/3}$ in $mkg^{-1/3}$ for Cylindrical Charges with **L/D Ratio of 5**. Horizontal Lines Indicate Shock Front Overpressure of Semispherical Charges of Identical Mass at the Same Scaled Distance.

Fig. 5.2b   Primary Shock Front Side-on Overpressure
as a Function of Azimuth Angle H and Scaled Distance
$Z = R \cdot Q^{-1/3}$ in mkg$^{-1/3}$ for Cylindrical Charges with
L/D Ratio of 5.   Horizontal Lines Indicate Shock Front
Overpressure of Semispherical Charges of Identical Mass
at the Same Scaled Distance.

Fig. 5.3    Side-on Overpressure - Impulse as a Function
of Azimuth Angle H and Scaled Distance Z in mkg $^{-1/3}$
for Cylindrical Charges with L/D Ratio of 1.
Horizontal Lines Indicate Impulses of Semispherical Charges
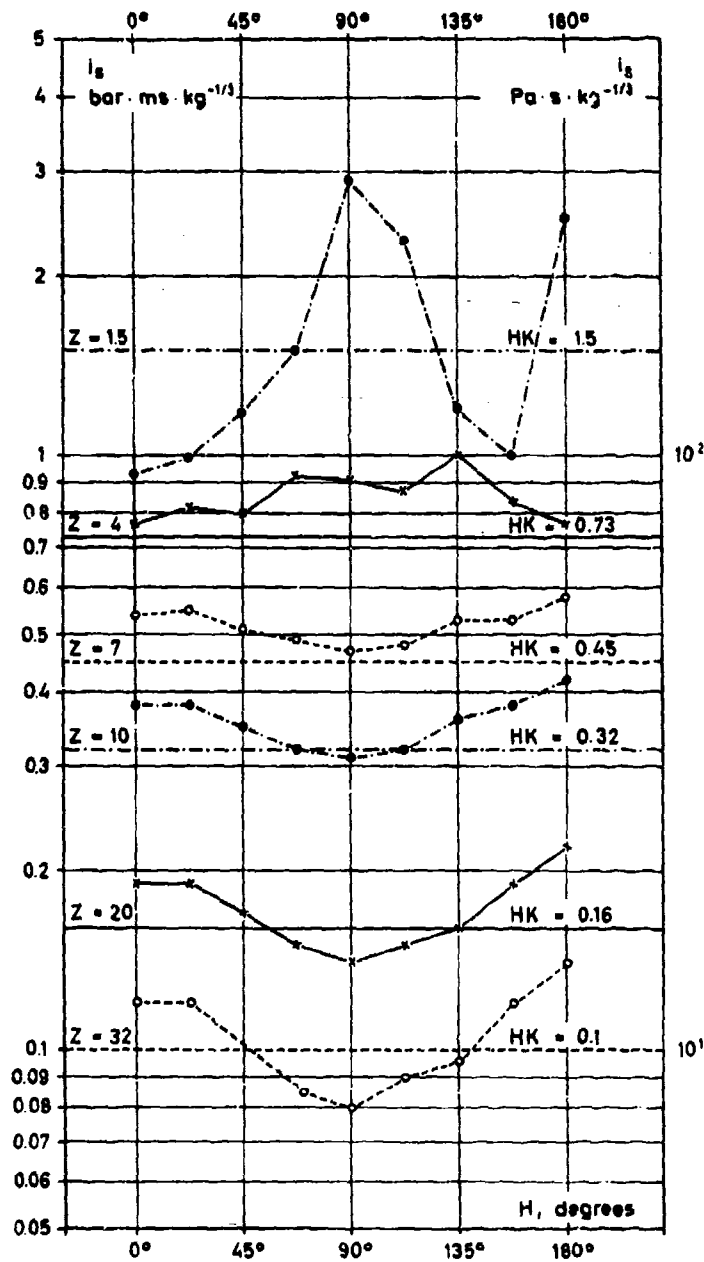of Identical Mass at the Same Scaled Distance.

106

Fig. 5.4 Side-on Overpressure - Impulse as a Function
of Azimuth Angle H and Scaled Distance Z in mkg^{-1/3}
for Cylindrical Charges with L/D Ratio of 5.
Horizontal Lines Indicate Impulses of Semispherical Charges
of Identical Mass at the Same Scaled Distance.

depends upon the impulse that is included in the first
pressure peak (not to be confused with the total over-
pressure impulse).

Figures 5.3 and 5.4 summarize total side-on overpressure
impulse for L/D = 1 and 5. Multiple shocks are included. It
is remarkable that at some distances blast impulses at the
surface of the ground show higher values at any direction
around a cylindrical charge than around a hemispherical
charge. Again this phenomenon may be explained by geometri-
cal effects, that the cylinder presents greater surface area
in the direction of the ground surface than the hemisphere.
Also blast impulses that show very high values in a certain
direction in the near field (e.g. $180^{\circ}$ in Fig. 5.4) tend to
fall down to rather low values at greater distances.

## 6. Blast Parameters versus Scaled Distance

The diagrams'-figures 6.1 to 6.4-contain a presentation of primary shock front peak overpressure versus scaled distance values and positive pressure impulse versus scaled distance values derived from our small scale measurements. The values of blast parameters in Ref. 4 were all scaled to a kilogram equivalent at standard sea level conditions. To use the curves for predicting blast data for other yields at other than standard sea level conditions standard scaling procedures should be used. This type of diagram has been used in Ref. 1 and may give the most complete presentation of our results.

As reference values results from semispherical charge detonations were fit into the diagrams that may make clear the big differences in peak overpressure in different directions around elongated charges. Kingery (Ref. 1) has fitted experimental peak overpressure data from hemispherical charges. The curve fit is of the functional form

$$P_S = f(Z)$$

$P_S$ = peak side-on overpressure

$Z$ = scaled distance.

Plooster (Ref. 5) has curve-fit the experimental peak side-on overpressure data obtained from a test program conducted at Denver Research Institute for cylindrical charges in free air. Much more data are needed in order to make a curve fit of the functional form

$$P_s = f(Z; L/D; H)$$

$P_s$ = peak side-on overpresure

$Z$ = scaled distance

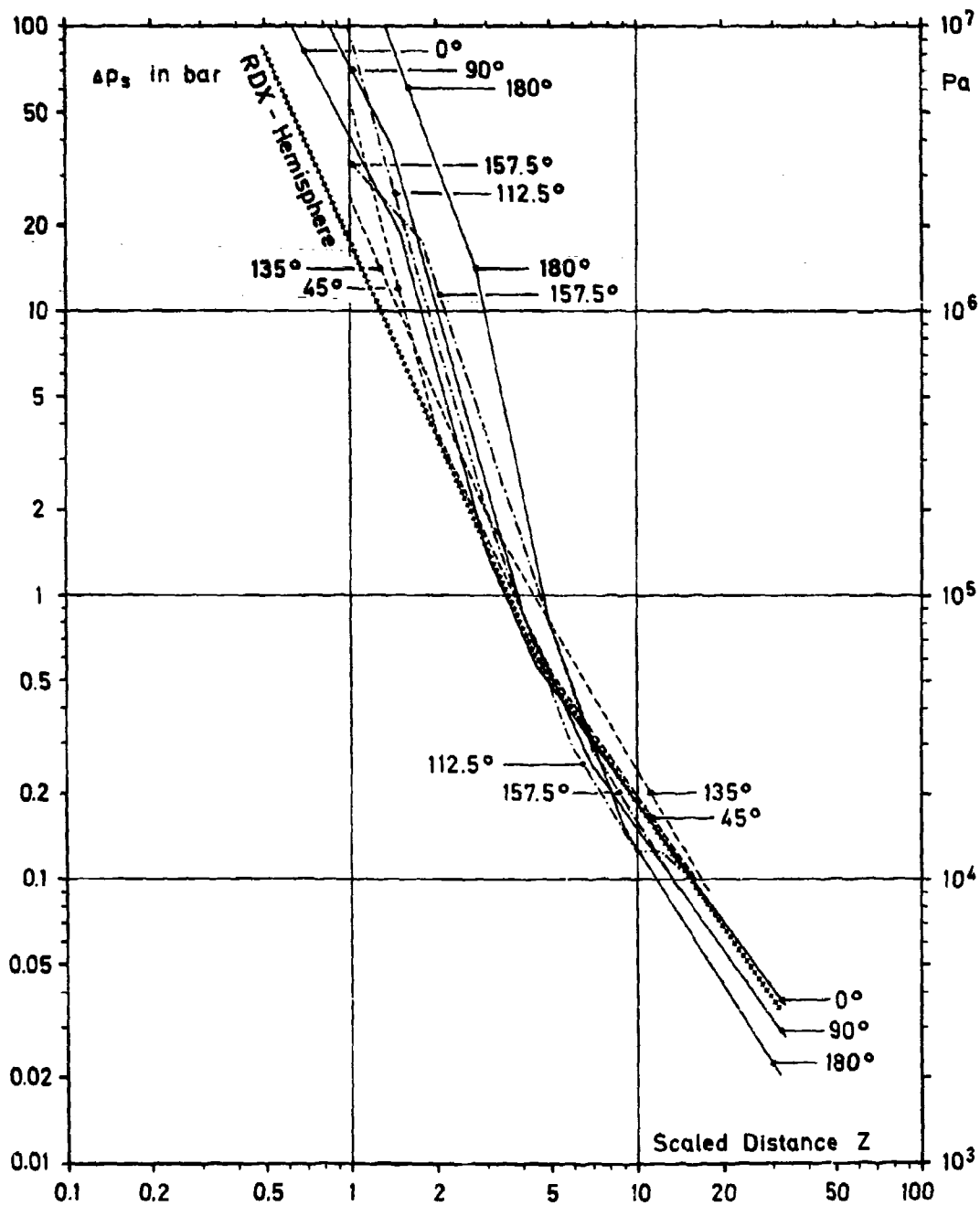$L/D$ = cylinder length to diameter ratio

$H$ = azimuth angle

109

Fig. 6.1
Primary Shock Front Overpressure vs. Scaled Distance
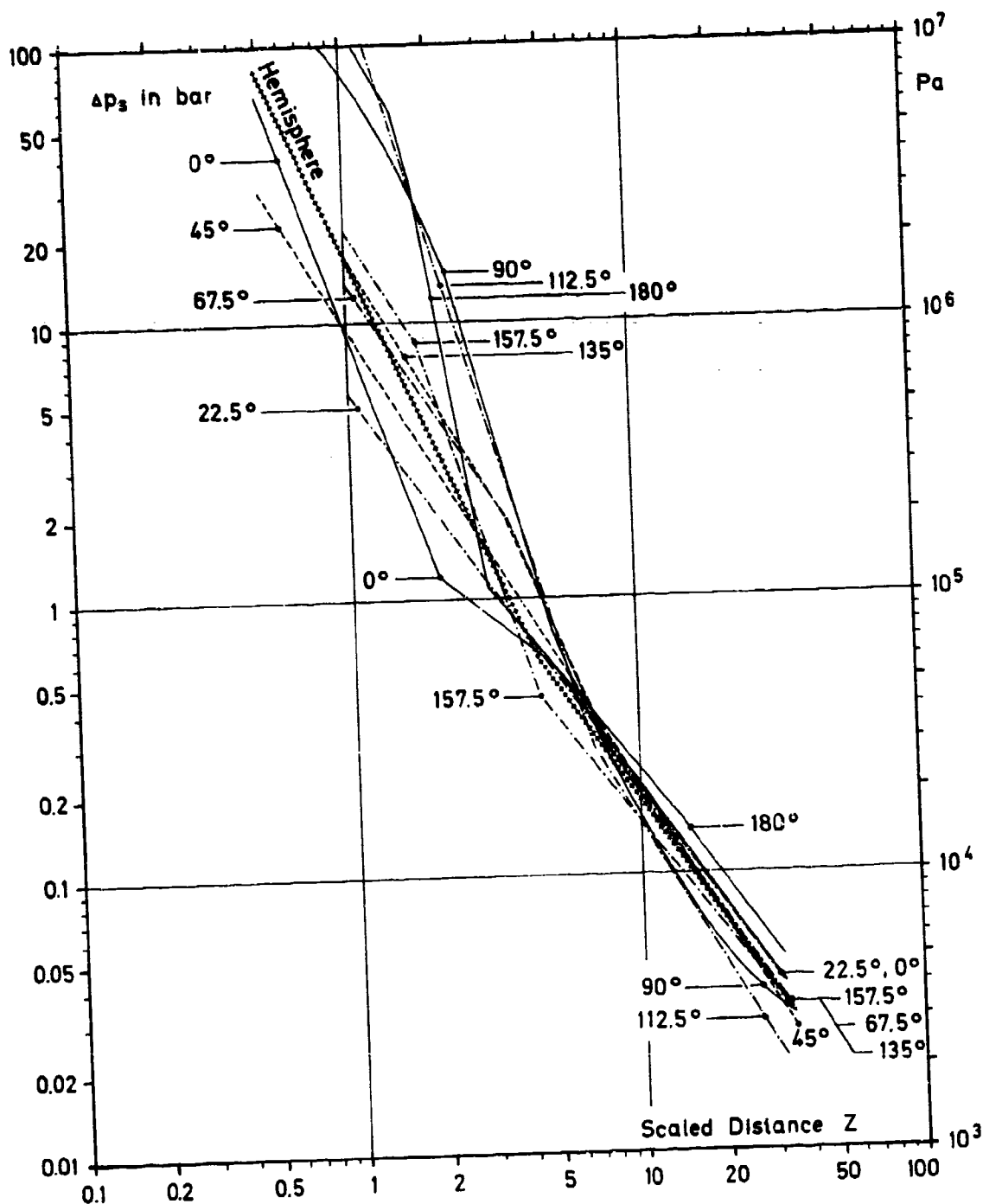for Cylindrical RDX Surface Bursts L/D = 1

Fig. 6.2
Primary Shock Front Overpressure vs. Scaled Distance
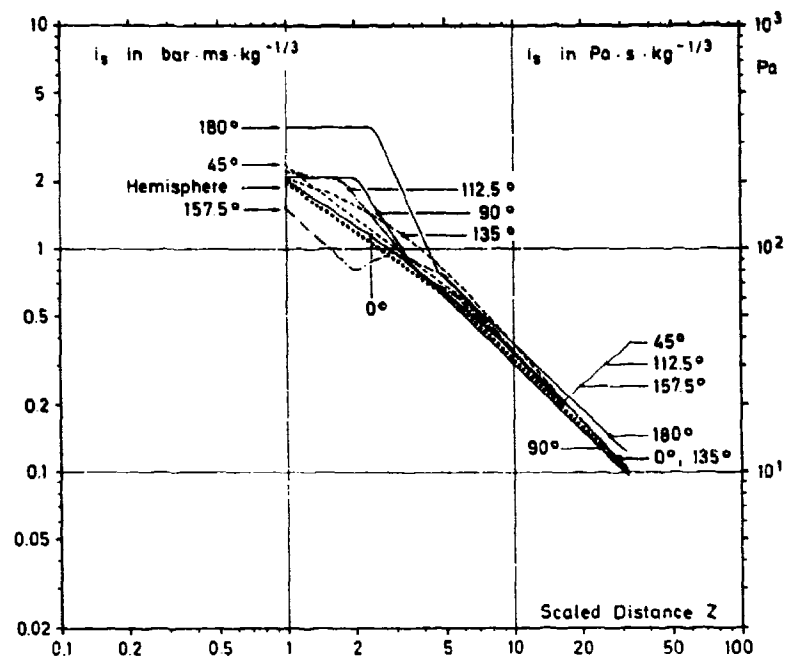for Cylindrical RDX Surface Bursts L/D = 5

111

Fig. 6.3    Overpressure - Impulse vs. Scaled Distance
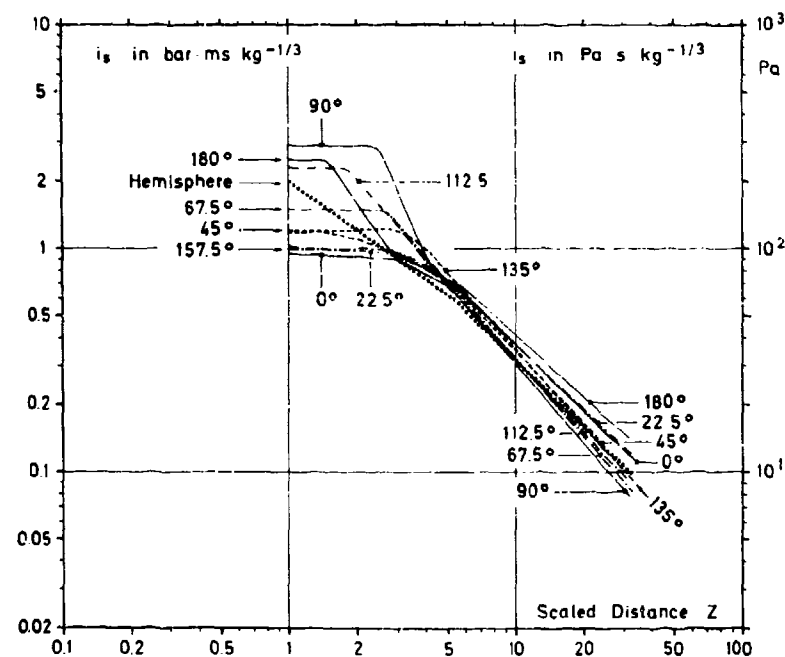for Cylindrical RDX Surface Bursts L/D = 1



Fig. 6.4    Overpressure - Impulse vs. Scaled Distance
for Cylindrical RDX Surface Bursts L/D = 5

112

Curve fitting of the data presented in this report has not
yet been completed. It is more complicated than in Ref. 5
as a wider range of distances, peak overpressures and blast
impulses was investigated.


7. References

1.    Kingery C.N., Pannill B.F.

      "Peak Overpressure vs Scaled Distance for TNT Surface
      Bursts (Hemispherical Charges)",  Ballistic Research
      Laboratories, Memorandum Report No. 1518, Apr. 1964

2.    Reisler R.E., Giglio-tos L., Teel G.D

      "Air Blast Parameters from Pentolite Cylinders
      Detonated on the Ground",  Ballistic Research Labora-
      tories, Memorandum Report No. 2471, Apr. 1975

3.    "A Manual for the Prediction of Blast and Fragment
      Loadings on Structures".  U.S. Department of Energy
      (prepared by Southwest Research Institute, San Antonio,
      Texas), DOE/TIC-11268, Nov. 1980

4.    Gürke G., Scheklinski-Glück G., Detterer M., Mehlin H.P.

      "Blastparameter bei der Oberflächendetonation von Ex-
      plosivstoffzylindern".  Bericht des Ernst-Mach-Instituts,
      No. E 6/82, März 1982

5.    Plooster M.N.

      "Blast Front Pressure from Cylindrical Charges of High
      Explosives",  Naval Weapons Center, Technical Memorandum
      No. 3631, Sept. 1978.